Non-stationary Equivariant Graph Neural Networks for Physical Dynamics Simulation

Chaohao Yuan^{1,2}*, Maoji Wen¹*, Ercan Engin Kuruoglu¹†, Yang Liu², Jia Li⁵,

Tingyang Xu^{3,4}, Deli Zhao³, Hong Cheng², Yu Rong^{3,4}†

¹ Tsinghua Shenzhen International Graduate School, Tsinghua University

² The Chinese University of Hong Kong

³ DAMO Academy, Alibaba Group ⁴ Hupan Lab,

⁵ Hong Kong University of Science and Technology (Guangzhou)

chaohaoyuan@link.cuhk.edu.hk, wmj24@mails.tsinghua.edu.cn,

kuruoglu@sz.tsinghua.edu.cn, yu.rong@hotmail.com

Abstract

To enhance the generalization ability of graph neural networks (GNNs) in learning and simulating physical dynamics, a series of equivariant GNNs have been developed to incorporate the symmetric inductive bias. However, the existing methods do not consider the non-stationarity nature of physical dynamics, where the joint distribution changes over time. Moreover, previous approaches for modeling nonstationary time series typically involve normalizing the data, which disrupts the symmetric assumption inherent in physical dynamics. To model the non-stationary physical dynamics while preserving the symmetric inductive bias, we introduce a Non-Stationary Equivariant Graph Neural Network (NS-EGNN) to capture the non-stationarity in physical dynamics while preserving the symmetric property of the model. Specifically, NS-EGNN employs Fourier Transform on segments of physical dynamics to extract time-varying frequency information from the trajectories. It then uses the first and second-order differences to mitigate non-stationarity, followed by pooling for future predictions. Through capturing varying frequency characteristics and alleviate the linear and quadric trend in the raw physical dynamics, NS-EGNN better models the temporal dependencies in the physical dynamics. NS-EGNN has been applied on various types of physical dynamics, including molecular, motion and protein dynamics, and consistently surpasses the existing state-of-the-art algorithms, underscoring its effectiveness. The implementation of NS-EGNN is available at https://github.com/MaojiWEN/NS-EGNN.

1 Introduction

Accurately simulating real-world physical dynamics is crucial in numerous fields, including molecular dynamics, motion capture [48], drug discovery [37, 54], and protein folding [1]. The challenge lies in capturing complex interactions among system components. However, traditional methods are either computationally expensive (e.g., Density Functional Theory [21]) or fail to model the complex human intention. Hence, various equivariant Graph Neural Networks (GNNs) [38, 16, 39, 18, 19, 24, 58, 26, 4, 57, 22, 5] have been developed to model such physical interactions while incorporating fundamental symmetry constraints. Specifically, these methods ensure their outputs are equivariant with respect to a specific group, such as E(3), any 3-dimensional translation/orientation/reflection.

^{*}Equal Contribution.

[†]Corresponding Authors

Despite their success, most existing models for physical dynamics focus on single-step frame-to-frame forecasting. That is, they only leverage a single historical frame as input to predict the future states. Such frameworks are insufficient to simulate physical dynamics due to the following issues: (1) **Non-Markovian**. According to the Markovian assumption, future states depend only on the current state and are independent of past states. However, a single frame of the physical dynamics does not comprehensively capture all the details of a given environment because of hidden interactions, such as those involving the solvent; (2) **Non-stationary**. Non-stationarity refers to a dynamic object whose statistical properties and joint distribution change over time. The time-varying distribution in physical dynamics can lead to poor generalization ability in deep learning models. More intuitively, in molecular dynamics, the potential energy of molecules are varying, which results the mean, variance (amplitude of vibration) and covariance (the connections between edges) change over time. Besides, in motion capture dataset, since velocity and physiological state are dynamic, the trajectories of human will also exhibit strong non-stationary property.

It is non-trivial to model Non-stationary and Non-Markovian dynamics. Previous works [28, 30, 52] for modeling non-stationary time-series data mostly adopt normalization approaches to stationarize the series. However, these methods will break the symmetry in the dynamics. An effective alternative, Fourier Transform [41] converts the physical dynamics from time domain to frequency domain, revealing the intensity of each frequency component within the dynamics. The frequency components and power spectrum in the frequency domain can be used to analyze the energy distribution of the physical dynamics [52], which in turn can be used to infer timedomain characteristics, such as variance. As illustrated in Figure 1, the Fourier frequency, S_1 , S_2 and S_3 , are distinct over different period, exhibiting the dynamic statistical property of dynamics in time domain.

In this paper, to incorporate the non-stationarity into the equivariant models, we propose Non-Stationary Equivariant Graph Neural Network (NS-EGNN), which adopts Fourier transform on patched physical dynamics to capture the varying distribution throughout the entire trajectory. Moreover, the Fourier frequency also reflects

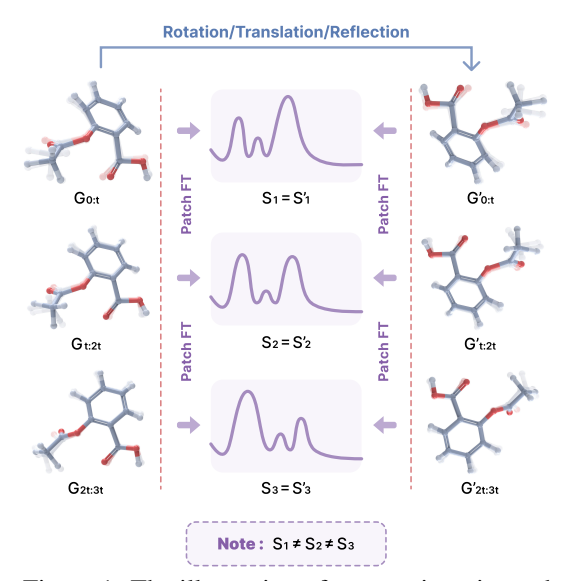


Figure 1: The illustration of non-stationarity and equivariance. **Non-stationarity:** Applying Fourier Transform (FT) to each period of dynamic object will result in different frequency pattern. **Invariance:** With rotation, translation or reflection of physical object, the model should capture the same frequency information.

the non-Markovian interactions inside the physical systems. Specifically, to capture the dynamic statistical properties inside the non-stationary physical objects, NS-EGNN segments patches of trajectory with overlap and applies Fourier transform to extract the time-varying frequency information from these dynamics. Notably, the extracted frequency features are E(3)-invariant, thus preserving the symmetric properties of the model. Subsequently, to capture the spatial relationships, NS-EGNN employs an equivariant GNN backbone to learn these spatial connections. Moreover, since the Patch Fourier Transform already captures the dynamic patterns, NS-EGNN does not additionally incorporate temporal learning modules, such as attention [47], thus achieving lower computational complexity. Finally, NS-EGNN performs multi-step prediction utilizing the updated spatio-temporal graph through the non-stationary temporal pooling module based on the first order and the second order differencing [32]. Our contributions are summarized as follows:

- We reveal the non-stationary property widely exists in real-world physical objects, such as molecules, proteins and human motions, via Augmented Dickey-Fuller (ADF) [46] test.
- We design a Non-Stationary Equivariant Graph Neural Network (NS-EGNN), leveraging Patch Fourier Transform with window function, to explicitly capture the time-varying frequency information in the dynamic object. Moreover, we design a novel equivariant temporal pooling layer to further alleviate the influence of non-statiaonarity.

 We apply NS-EGNN across various applications, such as molecular-, protein- and macro-level simulation. In the various scenarios, NS-EGNN consistently indicates performance improvements.

2 Background

2.1 Problem Definition

Notation. A physical object can be represented as a graph $\mathcal{G} = (\mathcal{V}, \mathcal{E}, \vec{\mathbf{X}})$. The node features $n_i \in \mathcal{V}$ include non-geometric features $\mathbf{h} \in \mathbb{R}^d$ such as the types of the atoms and a 3D coordinate vector $\vec{\mathbf{X}}_i \in \mathbb{R}^3$, and the edge features $e_{ij} \in \mathcal{E}, \in R^e$ describes the connection between node i and node j. In a historical trajectory of this object $\{\mathcal{G}\}_{t=0}^T$, the scalar features \mathbf{h} and edge features \mathbf{e} are constant while the position vectors $\vec{\mathbf{X}}$ change over time.

Task Definition. In the trajectory simulation task, given the past trajectory $\{\mathcal{G}\}_{t=0}^T$, the target is to learn a function f_{θ} that predicts the future trajectory $\{\mathcal{G}\}_{t=T+1}^{T+\Delta t}$.

$$\{\mathcal{G}\}_{t=T+1}^{T+\Delta t} = f_{\theta}(\{\mathcal{G}\}_{t=0}^{T}). \tag{1}$$

Specifically, since only the position vectors are dynamic, the primary focus is on predicting \vec{X} .

2.2 Equivariance and Invariance

In the group of E(3), the transformation $g \cdot \vec{\mathbf{X}}$ can be expressed as: $g \cdot \vec{\mathbf{X}} := \mathbf{O}\vec{\mathbf{X}} + \mathbf{t}$, where $\mathbf{O} \in \mathbf{O}(3) = \{\mathbf{O} \in \mathbb{R}^{3 \times 3} | \mathbf{O}^{\top} \mathbf{O} = \mathbf{I}\}$ represents orthogonal transformations (including rotation and reflection), and $\mathbf{t} \in \mathbb{R}^3$ represents translations.

Given above definitions, to enhance generalization ability, when a physical object undergoes transformations within the group E(3), the equivariant model f_{θ} should be able to produce the corresponding prediction for the coordinates. In the context of a spatio-temporal graph, this can be formulated as:

$$\{\mathcal{G} = (\mathcal{V}, \mathcal{E}, g \cdot \vec{\mathbf{X}})\}_{t=T+1}^{T+\Delta t} = f_{\theta}(\{\mathcal{G} = (\mathcal{V}, \mathcal{E}, g \cdot \vec{\mathbf{X}})\}_{t=0}^{T}).$$
(2)

2.3 Non-stationarity

A non-stationary time series exhibits dynamic statistical properties and joint distribution, resulting it difficult to be modeled by deep learning models [51, 36]. Formally, such property can be defined as:

Definition 1. (Non-stationary) Physical dynamics $\{\vec{\mathbf{X}}_t\}$ can be considered as non-stationary if there exists distinct time interval t_1 and t_2 such that at least one of the following conditions is met: $E(\vec{\mathbf{X}}_{t_1}) \neq E(\vec{\mathbf{X}}_{t_2})$, $Var(\vec{\mathbf{X}}_{t_1}) \neq Var(\vec{\mathbf{X}}_{t_2})$, or $Cov(\vec{\mathbf{X}}_{t_1}, \vec{\mathbf{X}}_{t_1+k}) \neq Cov(\vec{\mathbf{X}}_{t_2}, \vec{\mathbf{X}}_{t_2+k})$ for any lag k.

In other words, if the mean, variance, or covariance function of a physical object evolve over time, then the object is considered to be non-stationary. Furthermore, Fourier frequency also details how the variance of the data is distributed across different frequencies. In the following work, we will utilize this frequency information to model and capture the non-stationary characteristics.

3 Methodology

3.1 General Framework

As shown in Figure 2, given an EGNN backbone, NS-EGNN consists of Patch Fourier transform (PFT) (Section 3.1.1) and non-stationary pooling layer (NS-Pooling) (Section 3.1.2) to model the non-stationary dynamics equivariantly. Specifically, the brief procedure can be represented as:

$$s = PFT(\vec{\mathbf{X}}(t)), \tag{3}$$

$$h^{(L)}, s^{(L)}, (\vec{\mathbf{X}}(t)^{(L)})_{t=0}^{T} = \text{EGNN}(h, s, \vec{\mathbf{X}}(t)_{t=0}^{T}), \tag{4}$$

$$\vec{\mathbf{X}}^* = \text{NS-Pooling}((\vec{\mathbf{X}}(t)^{(L)})_{t=0}^T). \tag{5}$$

Here, $h^{(L)}, s^{(L)}, (\vec{\mathbf{X}(t)}^{(L)})_{t=0}^T$ denote the L-th EGNN layer output and $\vec{\mathbf{X}}^*$ is the final pooled trajectory. In PFT, we divide the trajectory into overlapping patches to capture the dynamic variance from the frequency domain, and in NS-Pooling, we employ a difference-based method to minimize the impact by dynamic mean and perform the multi-step prediction by pooling the stationarized dynamics. PFT and NS-Pooling model the dynamics' variance and mean, respectively. First, PFT extracts the invariant frequency features s from the input trajectory. These features, along with the original coordinates $\vec{\mathbf{X}}(t)_{t=0}^T$ and scalar features h, are fed into the EGNN [39] backbone, as delineated in Section 3.2, which updates the node states. Finally, the NS-Pooling layer is applied to the output coordinates $(\vec{\mathbf{X}}(t)^{(L)})_{t=0}^T$ from the EGNN to stationarize the features and make the final multi-step prediction $\vec{\mathbf{X}}^*$. Finally, the training objective of NS-EGNN is the mean square error (MSE) loss $\mathcal{L} = \sum_{t=T}^{T+T_L} \sum_{i=1}^{N} ||\vec{\mathbf{X}}_i^*(t) - \vec{\mathbf{X}}_i(t)||$.

3.1.1 Invariant Patch Fourier Transform

Discrete Fourier Transform (DFT). DFT is a classic algorithm that converts the trajectory from temporal domain to frequency domain, which contain the periodical information in the physical dynamics. Specifically, DFT \mathcal{F} can extract the frequency information $\vec{\mathbf{s}}_i \in \mathbb{C}^{T \times 3}$ of the physical dynamics at node i, and be calculated as follows:

$$\vec{\mathbf{s}}_i(k) = \mathcal{F}(\vec{\mathbf{X}}_i) = \sum_{t=0}^{T} e^{-i'\frac{2\pi}{T}kt} \cdot (\vec{\mathbf{X}}_i(t) - \bar{\vec{\mathbf{X}}}_i(t)),$$

where i' is the imaginary unit, $k = 0, 1, \dots, T$ is the frequency index and $\vec{X}_i(t)$ is the average position of all nodes in the graph. Nonetheless, DFT computes a single, global frequency spectrum for the entire trajectory, implicitly assuming the signal's properties are constant over time. We refer to this as *static frequency* information. Due to the inherent non-stationarity of physical dynamics, where statistical properties (and thus frequency components) change over time, this static spectrum is insufficient. Therefore, DFT cannot comprehensively capture the dynamic, time-varying frequency evolution inside the physical objects.

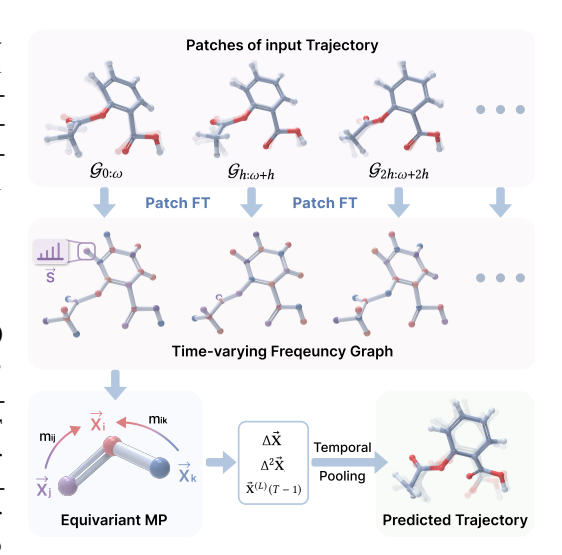


Figure 2: The overall framework of NS-EGNN. NS-EGNN applies window function to the input trajectory and Fourier Transform to receive timevarying frequency graphs. Then, the equivariant GNN will learn from both spatial and spectral information to update the coordinates.

Patch Fourier Transform (PFT). To this end, inspired by [15], we design the Patch Fourier Transform (PFT) to extract the frequency content of an object changes over time. Our target is to extract the Fourier frequency at each stage along the trajectory. However, directly cutting off parts of the trajectory can result in spectral leakage [35], which means it might not properly capture the frequency information. Therefore, PFT applies a window function $\mathbf{w}(\cdot;\omega)$ to accurately extract the local frequency in the segmented trajectory, where $\omega \in \mathbb{R}$ denotes window length as a hyperparameter, to determine the number of samples in each segment where Fourier transform is applied, defined as:

$$PFT(\vec{\mathbf{X}}_i)(p,k) = \sum_{t=0}^{T} e^{-i'\frac{2\pi}{T}kt} \cdot (\vec{\mathbf{X}}_i(t) - \bar{\vec{\mathbf{X}}}_i(t))\mathbf{w}(t - h \times p; \omega)$$
 (7)

where $p \in \mathbb{R}$ is the window index of Fourier transform applied, $k \in R$ denotes the frequency index in p-th window, and $h \in \mathbb{R}$ denotes the hop size, defined as the number of samples the window is moved forward at each time. Specifically, we adopt the classic Hamming window [35] $\mathbf{w}(t) = 0.54 - 0.46 \cdot \cos(\frac{2\pi t}{\omega - 1})$ as the window function. We also conduct an additional experiment in Appendix C.8 to prove the specific window function will not greatly influence the performance of NS-EGNN. By setting $h < \omega$, the windows overlap, allowing for more thorough capture of the frequency information throughout the trajectory.

Invariant Frequency Feature. To capture the entire frequency of physical dynamics, we applied the PFT to all dimensions of coordinates. In each dimension, PFT will result frequency matrix $\mathbf{S}_i \in \mathbb{R}^{r \times K}$, where r = T/h and $K \leq T$ is the number of frequency basis. To integrate the frequency information from different dimensions, the frequency features will be calculated as:

$$\mathbf{s} = \sqrt{\sum_{i=1}^{n} (|\mathbf{S}_i|^2)/n} \tag{8}$$

where n is the number of dimensions. We distribute the frequency feature s to each node involved in the Fourier transform calculation. Consequently, the dimension of s is extended to $\mathbb{R}^{T \times K}$, by repeating the feature h times. If a coordinate takes part in multiple Fourier transforms, its corresponding frequency feature will be averaged.

Multi-Scale PFT. On the other hand, to prevent the relatively small window size ω from limiting the ability to capture broader frequencies, we adopt a set of distinct window sizes and hop sizes in the implementation of NS-EGNN. By applying PFT q consecutive times with these varying hyperparameters, NS-EGNN can effectively capture different scales of frequency, enhancing its ability to model non-stationary trajectory. Hence, the final resulted frequency feature is given by $\mathbf{s} \in \mathbb{R}^{q \times T \times K}$.

Lemma 3.1. The extracted frequency feature **s** is E(n)-invariant.

The proof can be found in Appendix A.1. In our model, aside from using PFT, we do not incorporate additional temporal modules such as attention mechanisms as PFT already integrates temporal information. An ablation study is set up in Section 4.5. This further enhances efficiency, as the complexity of Fast FT is $O(N \log N)$, while the complexity of attention mechanism is $O(N^2)$, and this is further validated by empirical results in Appendix C.7.

3.1.2 Equivariant Non-stationary Temporal Pooling

Inspired by classical statistical algorithms [8], to reduce the non-stationary property, we propose NS-Pooling, to involve differencing the trajectory before pooling:

$$\Delta \vec{\mathbf{X}}_{i} = [\vec{\mathbf{X}}_{i}^{(L)}(1) - \vec{\mathbf{X}}_{i}^{(L)}(0), \vec{\mathbf{X}}_{i}^{(L)}(2) - \vec{\mathbf{X}}_{i}^{(L)}(1), \cdots, \vec{\mathbf{X}}_{i}^{(L)}(T-1) - \vec{\mathbf{X}}_{i}^{(L)}(T-2)]$$
(9)

where $\Delta \vec{\mathbf{X}}_i \in \mathbb{R}^{(T-1) \times 3}$ represents the differentiated. Furthermore, we also derive the second order difference $\Delta^2 \vec{\mathbf{X}}_i = \{\Delta \vec{\mathbf{X}}_i(t) - \Delta \vec{\mathbf{X}}_i(t-1)\}_{t=1}^{T-1}$. Although it is possible to derive higher-order differences, we find that first-order and second-order differences are sufficient for pooling. The corresponding experiments can be found in Appendix C.1. Moreover, while the previous works focused only on predicting the next single frame, our experiments extend the framework to a more challenge setting: forecasting the multi-step trajectory $\vec{\mathbf{X}}_i^* \in \mathbb{R}^{N \times \Delta t \times 3}$ of the physical dynamics, where Δt represents the length of the forecasted trajectory. The formulation can be represented as:

$$\vec{\mathbf{X}}_{i}^{*} = [\Delta \vec{\mathbf{X}}_{i}, \Delta^{2} \vec{\mathbf{X}}_{i}] \cdot \gamma + \vec{\mathbf{X}}_{i}^{(L)}(T-1), \tag{10}$$

where $\gamma \in \mathbb{R}^{(2T-3) \times T_L}$ is a learnable weight matrix. The differencing process removes linear and quadratic trends, making the trajectory more stationary and easier for the model to learn underlying patterns, rather than being distracted by absolute, non-stationary positions.

3.1.3 Equivariance Analysis

Let f_{θ} denote the overall NS-EGNN models, we have the theorem:

Theorem 3.2. For arbitrary orthogonal transformations and translation vectors $\mathbf{O}, \mathbf{t} \in E(3)$, $f_{\theta}(\{\mathbf{O}\mathcal{G} + \mathbf{t}\}_{t=0}^T) = \mathbf{O}f_{\theta}(\{\mathcal{G}\}_{t=0}^T) + \mathbf{t}$.

The proof is provided in the Appendix A.2. Since the composition of equivariant functions is again equivariant, the PFT module extracts invariant frequency features to feed into the an equivariant backbone. The NS-Pooling layer aggregates the first and second-order differences of the trajectory along with the final position, which is also equivariant.

3.2 Spatial Model Backbone

To process the spatial information in the dynamics, we leverage EGNN [39] layers μ as equivariant backbone in NS-EGNN framework. With the time-varying frequency feature s obtained by PFT, EGNN layers μ can iteratively update the system states as:

$$\mathbf{h}^{(l+1)}, \mathbf{s}^{(l+1)}, \vec{\mathbf{X}}^{(l+1)} = \mu(\mathbf{h}^{(l)}, \mathbf{s}^{(l)}, \vec{\mathbf{X}}^{(l)}), \tag{11}$$

where $\mathbf{h}_i^{(l)}$, $\mathbf{s}_i^{(l)}$ and $\vec{\mathbf{X}}_i^{(l)}$ are the scalar feature, frequency feature and geometric feature of node i at layer l, respectively. Specifically, EGNN employs relative distance $||\vec{\mathbf{X}}_i - \vec{\mathbf{X}}_j||$ as the invariant features:

$$\mathbf{m}_{ij}^{(l)} = f_{\theta}(\mathbf{h}_{i}^{(l)}, \mathbf{h}_{j}^{(l)}, \mathbf{s}_{i}^{(l)}, \mathbf{s}_{j}^{(l)}, ||\vec{\mathbf{X}}_{i}^{(l)} - \vec{\mathbf{X}}_{j}^{(l)}||^{2}), \tag{12}$$

where f_{θ} is an MLP and $\mathbf{m}_{ij}^{(l)}$ is the invariant message embedding between nodes i and j at l-th layer. Given the invariant message embedding, the node coordinates can be updated with equivariance:

$$\vec{\mathbf{X}}_{i}^{(l+1)} = \vec{\mathbf{X}}^{(l)} + \frac{1}{|\mathcal{N}_{i}|} \sum_{j \in \mathcal{N}_{i}}^{j \neq i} (\vec{\mathbf{X}}_{i}^{(l)} - \vec{\mathbf{X}}_{j}^{(l)}) \phi_{x}(\mathbf{m}_{ij}^{(l)}), \tag{13}$$

where ϕ_x denotes an MLP and \mathcal{N}_i is the neighbors of node i in the physical system. In terms of invariant features, with message embedding \mathbf{m} , the hidden representations \mathbf{h} and \mathbf{s} can be updated as:

$$\mathbf{h}_{i}^{(l+1)} = \mathbf{h}_{i}^{(l)} + \sum_{j \in \mathcal{N}_{i}}^{j \neq i} \phi_{h}(\mathbf{h}_{j}^{(l)}, \mathbf{m}_{ij}^{(l)}), \mathbf{s}_{i}^{(l+1)} = \mathbf{s}_{i}^{(l)} + \sum_{j \in \mathcal{N}_{i}}^{j \neq i} \phi_{s}(\mathbf{s}_{j}^{(l)}, \mathbf{m}_{ij}^{(l)}),$$
(14)

where f_{θ} , ϕ_h and are learnable neural networks.

While we here exploit EGNN [39] as the backbone, the patched dynamics modeling we proposed is a plug-and-play module that can be integrated into other models based on specific scenarios. For instance, in constrained and bounded physical systems, we could develop NS-GMN from GMN [19], and NS-DEGNN from DEGNN [58], respectively. We leave these extensions as future exploration.

4 Experiments

4.1 Experimental Settings

4.1.1 Datasets & Non-stationary Analysis

We perform experiments on three classic datasets: 1) MD17 [6], 2) CMU Motion Capture Database [7], and 3) AdK equilibrium trajectory dataset [40]. Note that these datasets all exhibit a strong non-stationary property. Specifically, the molecular and protein dynamics in the MD17 and AdK equilibrium trajectory datasets have varying potential energy, which influences the amplitude of vibration. In the motion capture dataset, the human's velocity and physiological state also vary over time.

To confirm the non-stationary nature of the datasets, we conduct Augmented Dickey-Fuller (ADF) tests [10] on each dataset. The ADF test quantifies the degree of stationarity by providing two primary metrics: the *p-value*, which reflects the significance of stationarity, and the *ADF statistic*, where smaller values indicate higher stationarity. Physical dynamics with p-values and ADF statistics below critical thresholds are deemed as stationarity, while higher values suggest the objects possess stronger non-stationary properties. More details can be found in Appendix B.1.

Table 1 summarizes the ADF test results for the MD17, CMU Motion Capture, and AdK

Table 1: Summarized ADF test results for MD17, CMU Motion Capture, and AdK datasets.

Non-Stat. Ratio	ADF Mean								
MD17 Da	taset								
0.8371	0.6684	-0.9185							
0.9997	0.9112	0.0896							
0.9427	0.4841	-1.4999							
0.9972	0.7741	-0.4416							
0.7710	0.3050	-2.0771							
0.9650	0.4540	-1.6494							
0.7840	0.2641	-2.2781							
0.4143	0.3161	-2.0884							
CMU Motion Cap	oture Dataset								
0.9601	0.8350	1.9866							
0.9449	0.7884	1.0581							
AdK Dataset									
0.4873	0.1739	-3.0586							
	MD17 Da 0.8371 0.9997 0.9427 0.9972 0.7710 0.9650 0.7840 0.4143 CMU Motion Cap 0.9661 0.9449 AdK Dat	MD17 Dataset 0.8371							

Table 2: Averaged prediction error for consecutive forecasts on the MD17 dataset. The reported mean and the standard deviation ($\times 10^{-3}$) are computed over 5 runs.

	Aspirin	Benzene	Ethanol	Malonaldehyde	Naphthalene	Salicylic	Toluene	Uracil
ST-TFN	$3.631_{\pm 0.136}$	$0.823_{\pm 0.007}$	$1.457_{\pm 0.083}$	$2.573_{\pm 0.071}$	$1.171_{\pm 0.061}$	$2.491_{\pm 0.198}$	$2.078_{\pm 0.097}$	$1.753_{\pm 0.037}$
ST-GNN	$10.509_{\pm 2.680}$	$1.833_{\pm 0.695}$	$14.349_{\pm 6.393}$	$4.066_{\pm0.461}$	$14.725_{\pm 1.265}$	$3.064_{\pm0.212}$	$2.401_{\pm 0.232}$	$2.324_{\pm 0.391}$
ST-SE(3)TR	$3.511_{\pm 0.167}$	$0.848_{\pm 0.035}$	$1.319_{\pm 0.006}$	$3.136_{\pm0.216}$	$1.063_{\pm 0.006}$	$2.858_{\pm 0.765}$	$2.669_{\pm 0.169}$	$1.754_{\pm 0.038}$
ST-EGNN	$3.257_{\pm 0.394}$	$0.876_{\pm0.144}$	$0.879_{\pm 0.112}$	$1.878_{\pm 0.258}$	$0.922_{\pm 0.063}$	$1.909_{\pm 0.320}$	$1.491_{\pm 0.139}$	$1.545_{\pm 0.152}$
EqMotion	$3.790_{\pm 0.018}$	$1.166_{\pm 0.279}$	$1.882_{\pm 0.011}$	$2.793_{\pm 0.013}$	$3.201_{\pm 0.008}$	$3.258_{\pm0.004}$	$2.917_{\pm 0.056}$	$3.288_{\pm0.002}$
STGCN	$4.175_{\pm 0.171}$	$1.001_{\pm 0.063}$	$214.904_{\pm 0.076}$	$3.455_{\pm0.370}$	$3.454_{\pm0.104}$	$3.433_{\pm 0.052}$	$3.110_{\pm0.131}$	$3.576_{\pm0.112}$
AGL-STAN	$587.048_{\pm 73.836}$	$5.914_{\pm 2.247}$	$303.185_{\pm 83.200}$	$53.283_{\pm 23.115}$	$33.055_{\pm 7.606}$	$3.256_{\pm0.310}$	$8.338_{\pm 1.475}$	$10.509_{\pm 0.351}$
ESTAG	$0.740_{\pm 0.059}$	$0.072_{\pm 0.014}$	$0.475_{\pm 0.020}$	$0.874_{\pm0.179}$	$0.405_{\pm 0.020}$	$0.636_{\pm0.100}$	$0.376_{\pm 0.043}$	$0.533_{\pm0.033}$
NS-EGNN	$0.421_{\pm 0.023}$	$0.050_{\pm 0.008}$	$0.410_{\pm 0.010}$	$0.589_{\pm 0.035}$	$0.275_{\pm 0.023}$	$0.387_{\pm 0.093}$	$0.308_{\pm 0.039}$	$0.379_{\pm 0.027}$

Table 3: Final prediction error for consecutive forecasts on the MD17 dataset. Bold font indicates the best result. The reported mean and the standard deviation ($\times 10^{-3}$) are computed over 5 runs.

	Aspirin	Benzene	Ethanol	Malonaldehyde	Naphthalene	Salicylic	Toluene	Uracil
ST-TFN	$6.026_{\pm 0.505}$	$1.615_{\pm 0.009}$	$2.051_{\pm 0.269}$	$4.596_{\pm 0.307}$	$1.436_{\pm 0.061}$	$3.571_{\pm 0.273}$	$2.700_{\pm 0.365}$	$2.893_{\pm 0.089}$
ST-GNN	$20.818_{\pm 7.168}$	$3.059_{\pm 0.513}$	$16.586_{\pm 6.768}$	$8.084_{\pm 1.017}$	$8.361_{\pm 5.020}$	$4.276_{\pm 1.172}$	$3.420_{\pm 0.140}$	$3.054_{\pm0.329}$
ST-SE(3)TR	$7.177_{\pm 1.037}$	$1.941_{\pm 0.672}$	$1.700_{\pm 0.029}$	$6.769_{\pm 0.599}$	$1.463_{\pm 0.049}$	$3.428_{\pm 0.629}$	$2.868_{\pm 0.183}$	$2.870_{\pm 0.083}$
ST-EGNN	$4.387_{\pm 0.635}$	$1.162_{\pm 0.238}$	$1.161_{\pm 0.100}$	$2.172_{\pm 0.678}$	$1.097_{\pm 0.126}$	$2.559_{\pm 0.307}$	$1.673_{\pm 0.315}$	$2.127_{\pm 0.328}$
EqMotion	$7.665_{\pm 0.056}$	$2.153_{\pm 0.064}$	$2.975_{\pm 0.011}$	$5.489_{\pm 0.005}$	$5.695_{\pm 0.036}$	$6.248_{\pm 0.012}$	$4.898_{\pm 0.011}$	$6.423_{\pm 0.122}$
STGCN	$7.628_{\pm 0.037}$	$2.008_{\pm0.037}$	$2.957_{\pm 0.015}$	$5.516_{\pm 0.047}$	$5.659_{\pm 0.038}$	$6.253_{\pm 0.040}$	$4.880_{\pm 0.006}$	$6.354_{\pm0.004}$
AGL-STAN	$634.663_{\pm 99.469}$	$6.028_{\pm 2.081}$	$271.624_{\pm 66.230}$	$58.795_{\pm 7.170}$	$29.899_{\pm 10.410}$	$3.798_{\pm 0.491}$	$8.418_{\pm 2.263}$	$10.085_{\pm 0.350}$
ESTAG	$1.446_{\pm 0.225}$	$0.169_{\pm 0.058}$	$0.898_{\pm 0.068}$	$1.442_{\pm 0.075}$	$0.801_{\pm 0.074}$	$1.038_{\pm 0.098}$	$0.730_{\pm 0.111}$	$1.086_{\pm0.150}$
NS-EGNN	$0.833_{\pm0.187}$	$0.147_{\pm 0.027}$	$0.695_{\pm0.020}$	$0.988_{\pm0.055}$	$0.598_{\pm0.149}$	$0.518_{\pm 0.026}$	$0.380_{\pm 0.056}$	$0.719_{\pm 0.219}$

datasets. For the MD17 dataset, molecules such as Benzene exhibit higher p-values and positive ADF statistics, reflecting pronounced non-stationary behavior. The CMU Motion Capture dataset's walk and run subsets show high p-values and positive ADF statistics, confirming their non-stationary nature. Lastly, the AdK dataset demonstrates substantial variability in its temporal dynamics, with approximately half of its nodes classified as non-stationary.

4.1.2 Baselines

We compare the performance of our proposed model with several widely used baselines in spatio-temporal trajectory modeling. STGCN [53] adopts a spatio-temporal convolutional architecture and is adjusted to predict residual coordinates between frames rather than absolute positions, as directly predicting the latter often leads to suboptimal performance. AGL-STAN [42], which combines adaptive graph learning with self-attention mechanisms, is modified to handle weighted temporal aggregation to better capture intra-temporal dependencies. ST-GNN [14], ST-SE(3)-Transformer [12], denoted as ST-SE(3)TR, ST-TFN [43], and ST-EGNN [39] are included as GNN baselines. Except for ST-GNN, which is based solely on the message passing framework, other approaches leverage rotational and translational invariance for trajectory prediction. Another representative model, EqMotion [48], integrates spatio-temporal information using attention-based fusion for modeling the object dynamics. ESTAG [47] first models the non-Markovian nature of physical dynamics and proposes an equivariant temporal attention module to capture the latent interaction. All baselines are modified to process the full historical trajectory (e.g., using linear encoders or, in the case of ESTAG, its native temporal attention) to ensure a fair comparison against our multi-step input model.

4.2 Molecular Dynamics

Setting. We evaluate the performance of our proposed model on the MD17 dataset, which includes molecular trajectories generated by MD simulation. The length of the input time series is set to 100, predicting the next 10 timesteps, with $\Delta t=5$, as time series requires more timesteps to observe non-stationarity. We also conduct the experiments with fewer timesteps in Appendix C.5, aligning with the setting in ESTAG, which also has satisfactory performance improvement. The dataset is split into training, validation, and testing sets with ratios of 0.2, 0.4, and 0.4, respectively.

Evaluation Metrics. We use two standard evaluation metrics: 1) Average Displacement Error (ADE), which measures the average ℓ_2 distance between the predicted and ground truth molecular trajectories over all timesteps. 2) Final Displacement Error (FDE), which evaluates the ℓ_2 distance between the predicted and ground truth positions at the final predicted step.

Results. Tables 2 and 3 summarize the ADE and FDE across all models. Notably, NS-EGNN emerges as the most effective model, surpassing baseline models considerably in both ADE and FDE metrics.

Table 4: Prediction error (MSE) for Walk ($\times 10^{-1}$) and Run ($\times 10^{0}$) cases under different time intervals (5ts, 10ts, 15ts, 20ts). The reported mean and standard deviation are computed over 5 runs.

Dataset			Walk ($\times 10^{-1}$)			Run (×10 ⁰)				
Time Itv.	5ts	10ts	15ts	20ts	Average	5ts	10ts	15ts	20ts	Average
ST-GNN	$1.121_{\pm 0.159}$	$1.224_{\pm 0.100}$	$2.615_{\pm 0.478}$	$3.359_{\pm 0.601}$	$1.941_{\pm 0.335}$	$0.560_{\pm 0.107}$	$1.160_{\pm 0.166}$	$1.538_{\pm 0.234}$	$1.779_{\pm 0.278}$	$1.259_{\pm 0.196}$
ST-TFN	$0.238_{\pm 0.032}$	$0.721_{\pm 0.038}$	$1.320_{\pm 0.067}$	$2.092_{\pm 0.094}$	$1.093_{\pm 0.058}$	$0.396_{\pm 0.073}$	$0.796_{\pm 0.054}$	$1.708_{\pm 0.318}$	$2.086_{\pm0.133}$	$1.247_{\pm 0.145}$
ST-SE(3)TR	$0.146_{\pm 0.017}$	$0.376_{\pm 0.097}$	$0.760_{\pm 0.161}$	$1.119_{\pm 0.347}$	$0.600_{\pm 0.156}$	$0.280_{\pm 0.045}$	$0.700_{\pm 0.131}$	$1.165_{\pm 0.267}$	$1.732_{\pm 0.550}$	$0.969_{\pm 0.248}$
ST-EGNN	$0.188_{\pm 0.026}$	$0.591_{\pm 0.103}$	$1.140_{\pm 0.123}$	$2.097_{\pm 0.205}$	$0.979_{\pm 0.114}$	$0.444_{\pm 0.072}$	$1.082_{\pm 0.113}$	$2.375_{\pm 0.202}$	$3.784_{\pm0.429}$	$1.921_{\pm 0.204}$
EqMotion	200020		-			$21.074_{\pm 2.073}$	$15.299_{\pm 4.127}$	$21.074_{\pm 2.073}$	$18.604_{\pm 3.503}$	$19.013_{\pm 2.944}$
STGCN	$0.302_{\pm 0.115}$	$0.828_{\pm0.203}$	$1.516_{\pm 0.384}$	$1.988_{\pm0.206}$	$1.159_{\pm 0.228}$	$0.131_{\pm 0.024}$	$0.582_{\pm 0.121}$	$1.101_{\pm 0.089}$	1.508 ± 0.176	$0.831_{\pm0.103}$
AGL-STAN	$1.729_{\pm 0.516}$	$1.789_{\pm 0.673}$	$2.030_{\pm 0.704}$	$2.155_{\pm 0.763}$	$1.926_{\pm 0.664}$	$0.511_{\pm 0.137}$	$0.628_{\pm 0.191}$	$0.648_{\pm 0.271}$	$0.831_{\pm 0.283}$	$0.654_{\pm 0.221}$
ESTAG	$0.054_{\pm 0.004}$	$0.213_{\pm 0.012}$	$0.530_{\pm 0.038}$	$1.085_{\pm 0.070}$	$0.471_{\pm 0.031}$	$0.041_{\pm 0.002}$	$0.250_{\pm 0.019}$	$0.771_{\pm 0.050}$	$1.767_{\pm 0.251}$	$0.707_{\pm 0.081}$
NS-EGNN	$0.051_{\pm 0.002}$	$0.166_{\pm 0.006}$	$0.397_{\pm 0.037}$	$0.775_{\pm 0.085}$	$0.347_{\pm 0.033}$	$0.033_{\pm 0.002}$	$0.187_{\pm 0.009}$	$0.584_{\pm 0.076}$	$1.226_{\pm 0.215}$	$0.508_{\pm 0.076}$

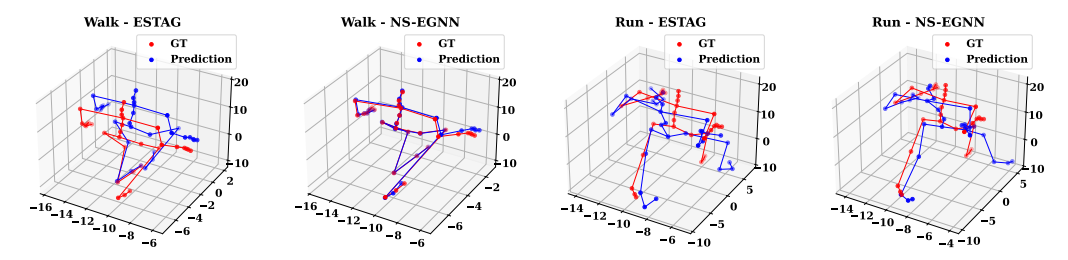


Figure 3: Visualization of predicted trajectories for run and walk motions at $time\ gap = 10$ and 20. Ground truth is represented in red, and predictions are in blue.

Specifically, compared with the current state-of-the-art model, NS-EGNN achieves an impressive relative improvement of 29.77% on ADE and 33.33% on FDE. Particularly with complex molecules like Aspirin and Malonaldehyde, NS-EGNN delivers an even more pronounced enhancement, reaching a 42.74% relative improvement for Aspirin. The second-best algorithm, which also utilizes a spatio-temporal approach to capture physical dynamics, underscores the importance of leveraging historical trajectory data. Nevertheless, NS-EGNN excels by explicitly modeling the dynamic statistical properties of physical objects, thereby achieving the best performance. Baseline models like STGCN and AGL-STAN exhibit high errors, as they are not equivariant. AGL-STAN's particularly poor performance, consistent with findings in other works [47], is due to its non-equivariant architecture struggling to model symmetric physical dynamics. Equivariant baselines such as ST-SE(3)TR and ST-EGNN perform better but are less robust in capturing the dynamic behaviors of larger molecules.

4.3 Motion Capture

Setting. CMU Motion Capture Database involves the trajectories of human motion under various scenarios. For this experiment, we focus on the *walk* and *run* motions, selecting trajectories with sufficient length. The input sequence consists of the past 10 frames used to predict the subsequent frame, with a data frame interval of $\Delta t = 1$. Additionally, we introduce a hyperparameter *time gap*, representing the delay between the last observed frame and the target frame to be predicted. Experiments are conducted with four values of *time gap*: 5ts, 10ts, 15ts, and 20ts. In *run* dataset, we additionally normalize the dataset, following previous works [47].

Results. Table 4 presents MSE across different models for both *walk* and *run* motions, indicating NS-EGNN consistently achieves the best performance in most settings. Specifically, NS-EGNN achieves an average improvement of **21.52%** in *walk* and **15.29%** in *run*, leading to an overall relative gain of **18.41%** across the entire dataset. This highlights the model's ability to capture the temporal and spatial dependencies crucial for human motion prediction. While AGL-STAN achieves the best performance in one case, NS-EGNN also remains highly competitive in that case. Overall, NS-EGNN demonstrates strong performance in both short-term and long-term predictions across different motions. Given that the motion dataset exhibits strong non-stationarity, it is not surprising that NS-EGNN achieves superior performance.

Visualization. Additionally, we provide visualizations of the predicted trajectories compared to the ground truth for both motions at *time gap* equals 10ts and 20ts, respectively. The visualizations, shown in Figure 3, include predictions from both ESTAG and our NS-EGNN. As illustrated, NS-EGNN predictions align more closely with the ground truth trajectories compared to ESTAG, particularly for complex joint movements. In the *walk* scenario, NS-EGNN exhibits smoother and more stable predictions, with trajectory paths closely following the ground truth points. For the *run*

motion, ESTAG struggles with maintaining coherence in the limb trajectories, resulting in noticeable distortions and erratic movements. In contrast, NS-EGNN better preserves the structural integrity of the motion, particularly in the torso and overall body posture, leading to a more realistic and physically plausible trajectory.

Table 5: Mean Squared Error (MSE) on the AdK dataset for protein dynamics prediction. The reported mean MSE values are computed over 5 runs. Bold font indicates the best result.

Model STGCN	ST-GNN	ST-EGNN	ST-GMN	AGL-STAN	ESTAG	NS-EGNN
MSE 3.007	2.267	1.751	1.743	1.853	1.758	1.738

4.4 Protein Dynamics

Setting. We evaluate our model on the AdK protein dynamics dataset, which involves predicting protein motions. For this dataset, we disable NS-pooling because it tends to overfit to noise. The input sequence consists of 60 timesteps used to predict the subsequent 10 timesteps, with $\Delta t = 5$. The dataset is split into training, validation, and testing sets with ratios of 0.6, 0.2, and 0.2, respectively. For consistency, all models are configured with 4 layers.

Results. Table 5 presents the MSE of all models on the AdK dataset. While the overall improvement margin is less pronounced than in previous experiments, NS-EGNN still achieves the best performance with an MSE of 1.738. This aligns with our findings from the ADF test (Table 1), where the AdK dataset exhibits a smaller proportion of non-stationary nodes compared to other datasets. As a result, the impact of explicitly addressing non-stationarity is naturally less significant. This further demonstrates NS-EGNN's generalization ability, allowing it to make accurate predictions even in datasets where non-stationary effects are less dominant.

Table 6: Ablation study results on the MD17 dataset. The table reports ADE values ($\times 10^{-3}$), averaged over three runs. Lower values indicate better performance.

Method	Aspirin	Benzene	Ethanol	Malonaldehyde	Naphthalene	Salicylic	Toluene	Uracil	Average
NS-EGNN	0.421	0.050	0.407	0.600	0.270	0.387	0.308	0.379	0.353
w/ Attention	0.499	0.039	0.389	0.751	0.280	0.446	0.317	0.377	0.387
w/o Patched FT	0.948	0.076	0.547	0.876	0.360	0.499	0.431	0.504	0.530
w/o Differentiation	2.622	0.265	0.700	1.929	0.949	2.249	1.103	1.448	1.408
w/o Equivariance	225.608	655.109	220.134	871.211	1365.762	10.397	281.836	7.861	454.740

4.5 The Effectiveness of Each Component in NS-EGNN

To evaluate the contributions of key components in NS-EGNN, we conduct experiments including or removing specific modules to analyze their impact, and results are in Table 6. From the table, we derive the following conclusions: 1) PFT extracts expressive temporal features. Prior work [47] introduced an equivariant temporal attention mechanism for learning physical dynamics. To explore potential improvements, we also incorporate this module. However, the overall performance shows a slight decline, suggesting that PFT already generates sufficiently expressive temporal features. 2) PFT is capable of capturing the dynamic statistic property in the non-stationary trajectory. We replace the PFT with a standard Fourier Transform applied to the entire trajectory. The observed worse performance suggests that PFT plays a critical role in modeling the temporal variance of non-stationary trajectories. This highlights the necessity of preserving localized frequency patterns. 3) Differentiation greatly reduces the negative impact of linear and quadric trend in the raw physical dynamics. The removal of this module results in a noticeable decline in performance, underscoring the critical role of differentiation in addressing mean shifts within non-stationary dynamics. Furthermore, without this component, the model loses crucial equivariant property. leading to suboptimal predictions. 4) Equivariant backbone enhances the generalization ability in dynamic simulation. The standard message passing GNN struggles to capture the symmetrical properties inherent in Euclidean space, leading to significantly poor performance. We further provide the NS-EGNN removing Fourier Transform entirely in Appendix C.4.

5 Related Works

Graph Neural Networks for Geometric Trajectory. TFN [43] and SE(3)-Transformer [12] employ spherical harmonics to extract high-order geometric representations. To reduce the computation in high-order representations, EGNN [39] updates invariant messages using relative distances and then derives directional vectors from these messages. For specific scenarios, many variants of EGNN [27] have been proposed, such as SGNN [17], GMN [19], DEGNN [58], EGHN [18] and EGNO [49]. EqMotion [48] and ESTAG [47] propose extracting the invariant and equivariant geometric features from historical dynamics, capturing temporal dependencies. However, these methods overlook the non-stationarity of physical dynamics, leading to suboptimal performance.

Non-stationarity in Time Series Forecasting. Before deep learning models, the classic ARIMA [3, 2] algorithm addressed non-stationarity by differencing the time series. The varying distribution of non-stationary data presents additional challenges for deep models. Pre-processing offers a straightforward and effective method to make the time series stationary. Adaptive Norm [33] normalizes fragment of the series according to the global statistics. Moreover, DAIN [34], RevIN [20], SAN [29], FAN [52], DDN [9] and IN-Flow [11] introduce learnable neural networks to normalize time series data. Furthermore, Transformers [28, 23, 13, 45, 44, 56, 55, 25] have been utilized to model non-stationary series with specialized attention mechanisms. However, direct stationarization of physical object coordinates of physical objects will unavoidably break the symmetric property of the deep models. To bridge this gap, NS-EGNN captures dynamic distributions while maintaining equivariance.

6 Conclusion

We show that trajectories of physical dynamics are highly non-stationary. Our NS-EGNN framework leverages the PFT and NS-Pooling modules to capture these patterns. By modeling non-stationary physical dynamics with equivariance, NS-EGNN greatly outperform the SOTA methods. A limitation is diminished gains on stationary data, where repeated FT increases computation with marginal benefits. Future work could extend NS-EGNN to domains to various settings and explore more spatial backbones [50] according to the specific scenarios. Furthermore, other methods for modeling non-stationary data, such as wavelet transforms, also break the equivariance. However, the adaption of these advanced method into equivariance also worth exploration.

Acknowledgments

This work is supported by Shenzhen Science and Technology Innovation Commission under Grant JCYJ20220530143002005, Tsinghua Shenzhen International Graduate School Start-up fund under Grant QD2022024C, Shenzhen Ubiquitous Data Enabling Key Lab under Grant ZDSYS20220527171406015, Damo Academy (Hupan Laboratory) through Damo Academy (Hupan Laboratory) Innovative Research Program, Damo Academy through Damo Academy Research Intern Program, Research Grants Council of the Hong Kong Special Administrative Region, China (No. CUHK 14217622), and Guangzhou Industrial Information and Intelligent Key Laboratory Project (No. 2024A03J0628). Additionally, Chaohao Yuan would like to thank his fiancée, Siying Xu, for her companionship and great help in visualization (Figure 1 & 2) in this work.

References

- [1] Bissan Al-Lazikani, Joon Jung, Zhexin Xiang, and Barry Honig. Protein structure prediction. *Current opinion in chemical biology*, 5(1):51–56, 2001.
- [2] George EP Box and Gwilym M Jenkins. Some recent advances in forecasting and control. *Journal of the Royal Statistical Society. Series C (Applied Statistics)*, 17(2):91–109, 1968.
- [3] George EP Box, Gwilym M Jenkins, Gregory C Reinsel, and Greta M Ljung. *Time series analysis: forecasting and control.* John Wiley & Sons, 2015.
- [4] Jiacheng Cen, Anyi Li, Ning Lin, Yuxiang Ren, Zihe Wang, and Wenbing Huang. Are high-degree representations really unnecessary in equivariant graph neural networks? *NeurIPS*, 37:26238–26266, 2024.

- [5] Jiacheng Cen, Anyi Li, Ning Lin, Tingyang Xu, Yu Rong, Deli Zhao, Zihe Wang, and Wenbing Huang. Universally invariant learning in equivariant gnns. arXiv preprint arXiv:2510.13169, 2025.
- [6] Stefan Chmiela, Alexandre Tkatchenko, Huziel E Sauceda, Igor Poltavsky, Kristof T Schütt, and Klaus-Robert Müller. Machine learning of accurate energy-conserving molecular force fields. *Science advances*, 3(5):e1603015, 2017.
- [7] CMU. Carnegie-mellon motion capture database, 2003. URL Lhttp://mocap.cs.cmu.edu.
- [8] Javier Contreras, Rosario Espinola, Francisco J Nogales, and Antonio J Conejo. Arima models to predict next-day electricity prices. *IEEE transactions on power systems*, 18(3):1014–1020, 2003.
- [9] Tao Dai, Beiliang Wu, Peiyuan Liu, Naiqi Li, Xue Yuerong, Shu-Tao Xia, and Zexuan Zhu. Ddn: Dual-domain dynamic normalization for non-stationary time series forecasting. *Advances in Neural Information Processing Systems*, 37:108490–108517, 2024.
- [10] Graham Elliott, Thomas J Rothenberg, and James H Stock. Efficient tests for an autoregressive unit root, 1992.
- [11] Wei Fan, Shun Zheng, Pengyang Wang, Rui Xie, Kun Yi, Qi Zhang, Jiang Bian, and Yanjie Fu. In-flow: Instance normalization flow for non-stationary time series forecasting. In *Proceedings of the 31st ACM SIGKDD Conference on Knowledge Discovery and Data Mining V. 1*, pages 295–306, 2025.
- [12] Fabian Fuchs, Daniel Worrall, Volker Fischer, and Max Welling. Se (3)-transformers: 3d roto-translation equivariant attention networks. *Advances in neural information processing systems*, 33:1970–1981, 2020.
- [13] Zidi Gao and Ercan Engin Kuruoglu. Attention based hybrid parametric and neural network models for non-stationary time series prediction. *Expert Systems*, 41(2):e13419, 2024.
- [14] Justin Gilmer, SamuelS. Schoenholz, Patrick Riley, Oriol Vinyals, and GeorgeE. Dahl. Neural message passing for quantum chemistry. *arXiv: Learning, arXiv: Learning*, Apr 2017.
- [15] Daniel Griffin and Jae Lim. Signal estimation from modified short-time fourier transform. *IEEE Transactions on acoustics, speech, and signal processing*, 32(2):236–243, 1984.
- [16] Jiaqi Han, Jiacheng Cen, Liming Wu, Zongzhao Li, Xiangzhe Kong, Rui Jiao, Ziyang Yu, Tingyang Xu, Fandi Wu, Zihe Wang, et al. A survey of geometric graph neural networks: Data structures, models and applications. *arXiv preprint arXiv:2403.00485*, 2024.
- [17] Jiaqi Han, Wenbing Huang, Hengbo Ma, Jiachen Li, Josh Tenenbaum, and Chuang Gan. Learning physical dynamics with subequivariant graph neural networks. *Advances in Neural Information Processing Systems*, 35:26256–26268, 2022.
- [18] Jiaqi Han, Wenbing Huang, Tingyang Xu, and Yu Rong. Equivariant graph hierarchy-based neural networks. *Advances in Neural Information Processing Systems*, 35:9176–9187, 2022.
- [19] Wenbing Huang, Jiaqi Han, Yu Rong, Tingyang Xu, Fuchun Sun, and Junzhou Huang. Equivariant graph mechanics networks with constraints. In *International Conference on Learning Representations*, 2022.
- [20] Taesung Kim, Jinhee Kim, Yunwon Tae, Cheonbok Park, Jang-Ho Choi, and Jaegul Choo. Reversible instance normalization for accurate time-series forecasting against distribution shift. In *International Conference on Learning Representations*, 2022.
- [21] Walter Kohn, Axel D Becke, and Robert G Parr. Density functional theory of electronic structure. *The journal of physical chemistry*, 100(31):12974–12980, 1996.
- [22] Zongzhao Li, Jiacheng Cen, Bing Su, Wenbing Huang, Tingyang Xu, Yu Rong, and Deli Zhao. Large language-geometry model: When Ilm meets equivariance. *arXiv preprint arXiv:2502.11149*, 2025.

- [23] Shizhan Liu, Hang Yu, Cong Liao, Jianguo Li, Weiyao Lin, Alex X. Liu, and Schahram Dustdar. Pyraformer: Low-complexity pyramidal attention for long-range time series modeling and forecasting. In *International Conference on Learning Representations*, 2022.
- [24] Yang Liu, Jiashun Cheng, Haihong Zhao, Tingyang Xu, Peilin Zhao, Fugee Tsung, Jia Li, and Yu Rong. SEGNO: Generalizing equivariant graph neural networks with physical inductive biases. In *The Twelfth International Conference on Learning Representations*, 2024.
- [25] Yang Liu, Zinan Zheng, Jiashun Cheng, Fugee Tsung, Deli Zhao, Yu Rong, and Jia Li. Cirt: Global subseasonal-to-seasonal forecasting with geometry-inspired transformer. In *ICLR*, 2025.
- [26] Yang Liu, Zinan Zheng, Yu Rong, and Jia Li. Equivariant graph learning for high-density crowd trajectories modeling. *Transactions on Machine Learning Research*, 2024.
- [27] Yang Liu, Zinan Zheng, Yu Rong, Deli Zhao, Hong Cheng, and Jia Li. Equivariant and invariant message passing for global subseasonal-to-seasonal forecasting. In KDD, pages 1879–1890, 2025.
- [28] Yong Liu, Haixu Wu, Jianmin Wang, and Mingsheng Long. Non-stationary transformers: Exploring the stationarity in time series forecasting. *Advances in Neural Information Processing Systems*, 35:9881–9893, 2022.
- [29] Zhiding Liu, Mingyue Cheng, Zhi Li, Zhenya Huang, Qi Liu, Yanhu Xie, and Enhong Chen. Adaptive normalization for non-stationary time series forecasting: A temporal slice perspective. *Advances in Neural Information Processing Systems*, 36:14273–14292, 2023.
- [30] Zhiding Liu, Mingyue Cheng, Zhi Li, Zhenya Huang, Qi Liu, Yanhu Xie, and Enhong Chen. Adaptive normalization for non-stationary time series forecasting: A temporal slice perspective. *Advances in Neural Information Processing Systems*, 36, 2024.
- [31] Ziqiao Meng, Liang Zeng, Zixing Song, Tingyang Xu, Peilin Zhao, and Irwin King. Towards geometric normalization techniques in se (3) equivariant graph neural networks for physical dynamics simulations. In *Proceedings of the Thirty-Third International Joint Conference on Artificial Intelligence*, pages 5981–5989, 2024.
- [32] Brian K Nelson. Time series analysis using autoregressive integrated moving average (arima) models. *Academic emergency medicine*, 5(7):739–744, 1998.
- [33] Eduardo Ogasawara, Leonardo C Martinez, Daniel De Oliveira, Geraldo Zimbrão, Gisele L Pappa, and Marta Mattoso. Adaptive normalization: A novel data normalization approach for non-stationary time series. In *The 2010 International Joint Conference on Neural Networks (IJCNN)*, pages 1–8. IEEE, 2010.
- [34] Nikolaos Passalis, Anastasios Tefas, Juho Kanniainen, Moncef Gabbouj, and Alexandros Iosifidis. Deep adaptive input normalization for time series forecasting. *IEEE transactions on neural networks and learning systems*, 31(9):3760–3765, 2019.
- [35] KM Muraleedhara Prabhu. Window functions and their applications in signal processing. Taylor & Francis, 2014.
- [36] Dayu Qin, Yi Yan, and Ercan Engin Kuruoglu. Llm-based online prediction of time-varying graph signals (student abstract). In *Proceedings of the AAAI Conference on Artificial Intelligence*, volume 39, pages 29472–29474, 2025.
- [37] A Srinivas Reddy, S Priyadarshini Pati, P Praveen Kumar, HN Pradeep, and G Narahari Sastry. Virtual screening in drug discovery-a computational perspective. *Current Protein and Peptide Science*, 8(4):329–351, 2007.
- [38] Alvaro Sanchez-Gonzalez, Jonathan Godwin, Tobias Pfaff, Rex Ying, Jure Leskovec, and Peter Battaglia. Learning to simulate complex physics with graph networks. In *International conference on machine learning*, pages 8459–8468. PMLR, 2020.
- [39] Victor Garcia Satorras, Emiel Hoogeboom, and Max Welling. E (n) equivariant graph neural networks. In *International conference on machine learning*, pages 9323–9332. PMLR, 2021.

- [40] Sean Seyler and Oliver Beckstein. Molecular dynamics trajectory for benchmarking MDAnalysis. 6 2017.
- [41] Ian Naismith Sneddon. Fourier transforms. Courier Corporation, 1995.
- [42] Mingjie Sun, Pengyuan Zhou, Hui Tian, Yong Liao, and Haiyong Xie. *Spatial-Temporal Attention Network for Crime Prediction with Adaptive Graph Learning*, page 656–669. Jan 2022.
- [43] Nathaniel Thomas, Tess Smidt, Steven Kearnes, Lusann Yang, Li Li, Kai Kohlhoff, and Patrick Riley. Tensor field networks: Rotation-and translation-equivariant neural networks for 3d point clouds. *arXiv preprint arXiv:1802.08219*, 2018.
- [44] Jiashan Wan, Na Xia, Yutao Yin, Xulei Pan, Jin Hu, and Jun Yi. Tcdformer: A transformer framework for non-stationary time series forecasting based on trend and change-point detection. *Neural Networks*, 173:106196, 2024.
- [45] Muyao Wang, Wenchao Chen, and Bo Chen. Considering nonstationary within multivariate time series with variational hierarchical transformer for forecasting. In *Proceedings of the AAAI Conference on Artificial Intelligence*, volume 38, pages 15563–15570, 2024.
- [46] Annette Witt, Jürgen Kurths, and A Pikovsky. Testing stationarity in time series. *physical Review E*, 58(2):1800, 1998.
- [47] Liming Wu, Zhichao Hou, Jirui Yuan, Yu Rong, and Wenbing Huang. Equivariant spatiotemporal attentive graph networks to simulate physical dynamics. *Advances in Neural Information Processing Systems*, 36, 2024.
- [48] Chenxin Xu, Robby T Tan, Yuhong Tan, Siheng Chen, Yu Guang Wang, Xinchao Wang, and Yanfeng Wang. Eqmotion: Equivariant multi-agent motion prediction with invariant interaction reasoning. In *Proceedings of the IEEE/CVF Conference on Computer Vision and Pattern Recognition*, pages 1410–1420, 2023.
- [49] Minkai Xu, Jiaqi Han, Aaron Lou, Jean Kossaifi, Arvind Ramanathan, Kamyar Azizzadenesheli, Jure Leskovec, Stefano Ermon, and Anima Anandkumar. Equivariant graph neural operator for modeling 3d dynamics. In *Proceedings of the 41st International Conference on Machine Learning*, pages 55015–55032, 2024.
- [50] Yi Yan and Ercan Engin Kuruoglu. Binarized simplicial convolutional neural networks. *Neural Networks*, 183:106928, 2025.
- [51] Yi Yan, Changran Peng, and Ercan E Kuruoglu. Graph signal adaptive message passing. *IEEE Signal Processing Letters*, 2025.
- [52] Weiwei Ye, Songgaojun Deng, Qiaosha Zou, and Ning Gui. Frequency adaptive normalization for non-stationary time series forecasting. In *The Thirty-eighth Annual Conference on Neural Information Processing Systems*, 2024.
- [53] Bing Yu, Haoteng Yin, and Zhanxing Zhu. Spatio-temporal graph convolutional networks: a deep learning framework for traffic forecasting. In *Proceedings of the 27th International Joint Conference on Artificial Intelligence*, pages 3634–3640, 2018.
- [54] Chaohao Yuan, Songyou Li, Geyan Ye, Yikun Zhang, Long-Kai Huang, Wenbing Huang, Wei Liu, Jianhua Yao, and Yu Rong. Annotation-guided protein design with multi-level domain alignment. In *Proceedings of the 31st ACM SIGKDD Conference on Knowledge Discovery and Data Mining V. 1*, pages 1855–1866, 2025.
- [55] Chaohao Yuan, Tingyang Xu, and Yu Rong. Transformer and drug design. In *Deep Learning in Drug Design*, pages 93–108. Elsevier, 2026.
- [56] Chaohao Yuan, Kangfei Zhao, Ercan Engin Kuruoglu, Liang Wang, Tingyang Xu, Wenbing Huang, Deli Zhao, Hong Cheng, and Yu Rong. A survey of graph transformers: Architectures, theories and applications. *arXiv* preprint arXiv:2502.16533, 2025.

- [57] Yuelin Zhang, Jiacheng Cen, Jiaqi Han, Zhiqiang Zhang, Jun Zhou, and Wenbing Huang. Improving equivariant graph neural networks on large geometric graphs via virtual nodes learning. In *ICML*, 2024.
- [58] Zinan Zheng, Yang Liu, Jia Li, Jianhua Yao, and Yu Rong. Relaxing continuous constraints of equivariant graph neural networks for broad physical dynamics learning. In *Proceedings of the 30th ACM SIGKDD Conference on Knowledge Discovery and Data Mining*, pages 4548–4558, 2024.

A Proofs

A.1 Proof of Lemma 3.1

Lemma 3.1 (,). The extracted frequency feature **s** is E(n)-invariant.

Proof. Recall Eq. 7,

$$PFT(\vec{\mathbf{X}}_i)(p,k) = \sum_{t=0}^{T} e^{-i'\frac{2\pi}{T}kt} \cdot (\vec{\mathbf{X}}_i(t) - \bar{\vec{\mathbf{X}}}_i(t))\mathbf{w}(t - h \times p; \omega)$$
(15)

After E(3) transformation, orthogonal O combined with translation t to the trajectory, the updated Fourier frequency is denoted as S_i^e :

$$\mathbf{S}_{i}^{e} = \sum_{t=0}^{T} e^{-i'\frac{2\pi}{T}kt} \cdot (\mathbf{O}\vec{\mathbf{X}}_{i}(t) + \mathbf{t} - \mathbf{O}\vec{\mathbf{X}}_{i}(t) - \mathbf{t})\mathbf{w}(t - h \times p; \omega)$$
(16)

$$= \sum_{t=0}^{T} e^{-i'\frac{2\pi}{T}kt} \cdot \mathbf{O}(\vec{\mathbf{X}}_{i}(t) - \bar{\vec{\mathbf{X}}}_{i}(t))\mathbf{w}(t - h \times p; \omega)$$
(17)

$$= \mathbf{O} \sum_{t=0}^{T} e^{-i'\frac{2\pi}{T}kt} \cdot (\vec{\mathbf{X}}_i(t) - \bar{\vec{\mathbf{X}}}_i(t)) \mathbf{w}(t - h \times p; \omega)$$
(18)

$$= \mathbf{OS}_i \tag{19}$$

We denote the transformed frequency feature as s^e with $OO^T = I$,

$$\mathbf{s}^e = \sqrt{\sum_{i=1}^n (|\mathbf{S}_i^e|^2)/n} \tag{20}$$

$$=\sqrt{\sum_{i=1}^{n}(|\mathbf{OS}_{i}|^{2})/n}\tag{21}$$

$$=\sqrt{\sum_{i=1}^{n}(|\mathbf{S}_{i}|^{2})/n}\tag{22}$$

$$= \mathbf{s}. \tag{23}$$

A.2 Proof of Theorem 3.2

Lemma A.1. Equivariant Message Passing is E(n)-equivariant.

Proof.

$$\mathbf{m}_{ij}^{(l)} = f_{\theta}(\mathbf{h}_{i}^{(l)}, \mathbf{h}_{j}^{(l)}, \mathbf{s}_{i}^{(l)}, \mathbf{s}_{j}^{(l)}, ||(\mathbf{O}\vec{\mathbf{X}}_{i}^{(l)} + \mathbf{t}) - (\mathbf{O}\vec{\mathbf{X}}_{j}^{(l)} + \mathbf{t})||^{2})$$
(24)

$$= f_{\theta}(\mathbf{h}_{i}^{(l)}, \mathbf{h}_{j}^{(l)}, \mathbf{s}_{i}^{(l)}, \mathbf{s}_{j}^{(l)}, ||\mathbf{O}(\vec{\mathbf{X}}_{i}^{(l)} - \vec{\mathbf{X}}_{j}^{(l)})||^{2})$$
(25)

$$= f_{\theta}(\mathbf{h}_{i}^{(l)}, \mathbf{h}_{j}^{(l)}, \mathbf{s}_{i}^{(l)}, \mathbf{s}_{j}^{(l)}, ||(\vec{\mathbf{X}}_{i}^{(l)} - \vec{\mathbf{X}}_{j})^{(l)}||^{2})$$
(26)

$$\mathbf{O}\vec{\mathbf{X}}_{i}^{(l+1)} + \mathbf{t} = \mathbf{O}\vec{\mathbf{X}}^{(l)} + \mathbf{t} + \frac{1}{|\mathcal{N}_{i}|} \sum_{j \in \mathcal{N}_{i}}^{j \neq i} (\mathbf{O}\vec{\mathbf{X}}_{i}^{(l)} + \mathbf{t} - \mathbf{O}\vec{\mathbf{X}}_{j}^{(l)} - \mathbf{t})\phi_{x}(\mathbf{m}_{ij}^{(l)}).$$
(27)

$$= \mathbf{O}(\vec{\mathbf{X}}^{(l)} + \frac{1}{|\mathcal{N}_i|} \sum_{j \in \mathcal{N}_i}^{j \neq i} (\vec{\mathbf{X}}_i^{(l)} - \vec{\mathbf{X}}_j^{(l)}) \phi_x(\mathbf{m}_{ij}^{(l)})) + \mathbf{t}$$
(28)

Lemma A.2. Equivariant Temporal Pooling is E(n)-equivariant.

Proof.

$$\vec{\mathbf{X}}_{i}^{*} = [\Delta \vec{\mathbf{X}}_{i}, \Delta^{2} \vec{\mathbf{X}}_{i}] \cdot \gamma + \vec{\mathbf{X}}_{i}^{(L)}(T-1). \tag{29}$$

With orthogonal transformation O and translation t in E(n) group.

$$\mathbf{O}\Delta \vec{\mathbf{X}}_i = \{\mathbf{O}\vec{\mathbf{X}}_i(t) + \mathbf{t} - \mathbf{O}\vec{\mathbf{X}}_i(t-1) - \mathbf{t}\}_{t=1}^T$$
(30)

$$= \mathbf{O}\{\vec{\mathbf{X}}_{i}(t) - \vec{\mathbf{X}}_{i}(t-1)\}_{t=1}^{T}$$
(31)

$$\mathbf{O}\Delta^{2}\vec{\mathbf{X}}_{i} = \mathbf{O}\{\Delta\vec{\mathbf{X}}_{i}(t) - \Delta\vec{\mathbf{X}}_{i}(t-1)\}_{t=0}^{T-1}$$
(32)

$$= \{\mathbf{O}\Delta\vec{\mathbf{X}}_i(t) - \mathbf{O}\Delta\vec{\mathbf{X}}_i(t-1)\}_{t=0}^{T-1}$$
(33)

Then, we have

$$\mathbf{O}\vec{\mathbf{X}}_{i}^{*} + \mathbf{t} = [\mathbf{O}\Delta\vec{\mathbf{X}}_{i}, \mathbf{O}\Delta^{2}\vec{\mathbf{X}}_{i}] \cdot \gamma + \mathbf{O}\vec{\mathbf{X}}_{i}^{(L)}(T-1) + \mathbf{t}$$

$$\Box$$
(34)

Theorem 3.2 (,). For arbitrary orthogonal transformations and translation vectors $\mathbf{O}, \mathbf{t} \in E(3)$, $f_{\theta}(\{\mathbf{O}\mathcal{G} + \mathbf{t}\}_{t=0}^T) = \mathbf{O}f_{\theta}(\{\mathcal{G}\}_{t=0}^T) + \mathbf{t}$.

Proof. As shown in Lemma 3.1, Lemma A.1, and Lemma A.2, since extracted spectral feature is invariant, and the rest of two components, Equivariant Message Passing and Equivariant Temporal Pooling, are equivariant, the model, $f_{\theta}(\cdot)$, is equivariant as well.

B Implementation Details

B.1 More Details on ADF Test

To provide a more comprehensive view of the Augmented Dickey-Fuller (ADF) test results, we present additional statistical measures that are omitted in the main paper for brevity.

To mitigate the influence of outliers, we exclude the top and bottom 3% of values when computing the mean and standard deviation of the ADF test metrics. For each node's spatial coordinates x,y,z, we determine the stationarity individually. A node is classified as non-stationary if any of its x,y,z or z dimensions fails the stationarity test. This ensures a comprehensive evaluation of the node's temporal behavior across all spatial dimensions.

Table 8 provides detailed statistics for each dataset, including the total number of trajectories, the count of non-stationary trajectories, the mean and standard deviation of the p-value, as well as the mean and standard deviation of the ADF statistic.

Table 7: Critical values for the ADF test across different datasets. Each column represents the 1%, 5%, and 10% significance thresholds.

Dataset	Mean 1%	Mean 5%	Mean 10%
MD17	-3.444	-2.868	-2.570
Motion Walk	-5.0538	-3.5246	-2.858
Motion Run	-5.0896	-3.5391	-2.8633
AdK	-3.5521	-2.9144	-2.5949

Table 7 lists the critical values used in the ADF test across different significance levels (1%, 5%, and 10%) for various datasets. If the ADF statistic of a time series is lower than the critical value at a given significance level, the null hypothesis of non-stationarity is rejected, confirming stationarity.

Table 8: Detailed ADF test results for the MD17, CMU Motion Capture, and AdK datasets. Each row summarizes key statistical measures for different subsets.

Subset	Total Trajectories	Non-Stationary Trajectories	Mean p-value	Std p-value	Mean ADF Statistic	Std ADF Statistic
		MD1	7 Dataset			
Aspirin	6500	5441	0.6684	0.2641	-0.9185	1.0372
Benzene	3000	2999	0.9112	0.1233	0.0896	0.8995
Ethanol	1500	1414	0.4841	0.3082	-1.4999	1.0187
Malonaldehyde	2500	2493	0.7741	0.2464	-0.4416	1.1369
Naphthalene	5000	3855	0.305	0.1944	-2.0771	0.5945
Salicylic	5000	4825	0.454	0.2541	-1.6494	0.7126
Toluene	3500	2744	0.2641	0.2343	-2.2781	0.8181
Uracil	4000	1657	0.3161	0.2293	-2.0884	0.7278
		CMU Motion	n Capture Datase	et		
Basketball	74400	71674	0.8507	0.2811	2.0209	3.7188
Walk	71300	68452	0.835	0.2907	1.9866	3.7633
Run	17050	16110	0.7884	0.3216	1.0581	3.2393
		AdI	K Dataset			
AdK	818133	401936	0.1761	0.2493	-3.0401	1.2173

The additional data in Table 8 further supports the non-stationary characteristics observed in the datasets. In particular, the MD17 dataset exhibits higher p-values in certain molecules (e.g., Benzene), indicating stronger non-stationary behavior. The CMU Motion dataset also demonstrates significant non-stationary characteristics, particularly in the basketball and walking sequences, where the mean ADF statistics are relatively high. The AdK dataset shows a relatively low mean p-value, indicating weaker stationarity.

The combination of these statistics and the stationarity assessment approach provides a robust framework for analyzing non-stationary characteristics in various datasets.

B.2 Hyperparameter Settings

This section presents the hyperparameter configurations used for training on different datasets. Table 9 summarizes the settings for MD17, CMU Motion, and AdK Protein datasets. The same model architecture is used across all datasets, but specific training configurations, such as the number of epochs, learning rate, and dataset splits, are adjusted to suit the characteristics of each dataset.

Table 9 presents the hyperparameter settings for each dataset. The learning rate and weight decay values are chosen based on dataset characteristics, with AdK Protein requiring a lower learning rate due to its complexity. The CMU Motion dataset contains different train-validation-test splits for walk and run, which are provided separately in the table. The number of layers, hidden dimension, and weight decay remain consistent across all datasets.

B.3 Compute Resources

All experiments reported in this paper were run on a dedicated high-performance server. The system is equipped with a single Intel® Xeon® Platinum 8358P CPU clocked at 2.60 GHz (32 cores, 64

Table 9: Hyperparameter configurations for different datasets. The dataset splits for CMU Motion are provided separately for *walk* and *run*.

Hyperparameter	MD17	CMU Motion	AdK Protein
Epochs	500	500	150
Learning Rate (lr)	5×10^{-3}	5×10^{-3}	5×10^{-5}
Weight Decay	1×10^{-12}	1×10^{-12}	1×10^{-12}
Number of Layers	4	4	4
Δ Frame	5	1	5
Hidden Dimension	16	16	16
Train/Val/Test Split	[2:4:4]	walk: [22:12:12] run: [5:4:2]	[6:2:2]

threads), 251 GiB of DDR4 main memory, and four NVIDIA H20 GPUs (each with 96 GiB of VRAM). We used NVIDIA driver version 550.120 and CUDA 12.4. This configuration remained constant across all training and evaluation runs.

Table 10: Compute resources used for all experiments.

Resource	Specification
CPU	Intel(R) Xeon(R) Platinum 8358P @ 2.60 GHz
	1 socket, 32 cores/socket (64 threads)
Memory	251 GiB DDR4 RAM
GPUs	$4 \times NVIDIA H20$
	96 GiB HBM3 VRAM each, 4.0 TB/s bandwidth
Driver	NVIDIA driver 555.50
CUDA	CUDA 12.4

C More Experimental Results

C.1 Experiments on Differential Orders

We further conduct the experiments incorporating each order differences in Table 11, and higher order information may lead potential over-fitting in the deep model and result suboptimal performance. Hence, in ES-NGNN, we only incorporate 1st-order and 2nd-order differencing.

Table 11: The experiments on incorporating different orders while pooling.

	Aspirin	Benzene	Ethanol	Malonaldehyde	Naphthalene	Salicylic	Toluene	Uracil	Average
None(ESTAG)	0.677	0.086	0.422	0.632	0.328	0.629	0.369	0.366	0.439
1st	0.467	0.726	0.419	0.634	0.368	0.45	0.33	0.381	0.39
2nd	0.421	0.05	0.407	0.6	0.27	0.387	0.308	0.379	0.353
3rd	0.501	0.058	0.408	0.583	0.273	0.341	0.3	0.4	0.358
4th	0.509	0.067	0.419	0.607	0.302	0.352	0.278	0.425	0.37

C.2 Ablations study that completely omitting Fourier Transform

Table 12: The ablation studies on removing PFT but keeping FT and completely omitting the FT.

	Aspirin	Benzene	Ethanol	Malonaldehyde	Naphthalene	Salicylic	Toluene	Uracil	Average
NS-EGNN	0.421	0.05	0.407	0.6	0.27	0.387	0.308	0.379	0.353
NS-EGNN w/o PFT	0.948	0.076	0.547	0.876	0.360	0.499	0.431	0.504	0.530
NS-EGNN w/o FT	0.564	0.062	0.436	0.619	0.385	0.425	0.358	0.467	0.480

We further conduct the ablation study that completely omitting the FT. The results are shown in Table 12. Surprisingly, we find totally remove FT even can outperform EGNN with FT, which indicates FT cannot accurately extract the intrinsic spectral information. The experiments demonstrates this inaccurate spectral feature also harms the convergence of the model.

C.3 Additional non-stationary and equivariant normalization baselines

C.4 Ablations study that completely omitting Fourier Transform

equivariant normalization [31]

C.5 Experiments on Original Settings in ESTAG

We further present the results of the original setting of ESTAG in Table 14. NS-EGNN still outperforms ESTAG in 7 out of 8 cases under the settings in ESTAG, achieving 10.3% relative performance improvement in average.

Table 13: The ablation studies on removing PFT but keeping FT and completely omitting the FT.

	Aspirin	Benzene	Ethanol	Malonaldehyde	Naphthalene	Salicylic	Toluene	Uracil	Average
NS-EGNN	0.421	0.05	0.407	0.6	0.27	0.387	0.308	0.379	0.353
EGNN w/normalization	4.286	1.238	1.298	4.661	1.084	1.824	0.762	1.471	2.078
Non-stationary Transformer	773.835	351.856	526.389	853.422	1449.999	18.570	290.497	9.793	531.483

Table 14: The performance (MSE) of NS-EGNN in the setting of ESTAG.

	Aspirin	Benzene	Ethanol	Malonaldehyde	Naphthalene	Salicylic	Toluene	Uracil	Average
ESTAG	0.063	0.003	0.099	0.101	0.068	0.047	0.079	0.066	0.068
NS-EGNN	0.052	0.003	0.097	0.100	0.059	0.057	0.065	0.058	0.061

C.6 Sensitivity of the Hyperparameters

Since the window length must be a factor of the number of past frames, and the hop length is typically selected as half of the window length to effectively capture dynamic frequencies, we explored various combinations of hop lengths for NS-EGNN, which applies PFT multiple times with different window lengths. The combinations are outlined as in Table 15.

Table 15: The ADE results of NS-EGNN with different set of hop length on MD17 dataset.

Нор	Aspirin	Benzene	Ethanol	Malonaldehyde	Naphthalene	Salicylic	Toluene	Uracil	Average
[2, 5, 10]	0.497	0.044	0.378	0.585	0.261	0.37	0.286	0.346	0.346
[5, 10, 20]	0.421	0.05	0.407	0.6	0.27	0.387	0.308	0.379	0.353
[10, 20, 50]	0.446	0.049	0.392	0.627	0.35	0.458	0.329	0.345	0.374

As observed in Table 15, these hyperparameters do not significantly impact the overall model performance.

C.7 Complexity and Epoch Training Time

Theoretically, the attention mechanism requires $O(N^2)$ complexity, while the Fast Fourier Transform (FFT) only requires $O(N\log N)$ complexity. Experimentally, we measured the average per-epoch training time (in milliseconds) of NS-EGNN and the baselines on the MD17 dataset across seven molecules. The results in Table 16 indicate that NS-EGNN is the most efficient algorithm compared with the baselines.

C.8 Sensitivity of Window Function

We further conduct the experiments on Blackman and Hann window functions on MD17 in Table 17. As observed in Table 17, NS-EGNN is insensitive to the type of window function. Additionally, the worst performance in the Table still outperforms all the baselines.

D Limitation

On the ADK dataset, our method shows smaller improvements than on MD17 and CMU Motion. This happens because our approach is designed for non-stationary data and is less effective when the data are more stationary.

E Broader Impacts

Our work contributes to more accurate and efficient dynamics simulations.

Broader impacts include:

- Accelerating drug discovery: Faster, more accurate simulations can reduce time and cost in identifying candidate compounds.

Table 16: Average epoch training time (ms) on MD17.

Method	Aspirin	Benzene	Ethanol	Malonaldehyde	Naphthalene	Salicylic	Toluene	Uracil	Average
ESTAG	40.3	21.1	12.9	17.5	32.7	32.6	23.8	21.8	25.34
Eqmotion	159.0	157.9	17.2	142.5	160.3	160.3	161.6	120.8	134.95
AGL-STAN	299.4	305.1	281.9	277.5	281.9	281.5	280.4	219.8	278.44
NS-EGNN	20.7	12.5	11.0	11.4	18.0	17.9	13.8	13.3	14.83

Table 17: The impact of different window functions on MD17 dataset.

Window	Aspirin	Benzene	Ethanol	Malonaldehyde	Naphthalene	Salicylic	Toluene	Uracil	Average
Hamming	0.409	0.038	0.389	0.584	0.32	0.338	3.291	0.331	0.337
Blackman	0.445	0.046	0.389	0.59	0.244	0.365	0.281	0.374	0.342
Hann	0.421	0.05	0.407	0.6	0.27	0.387	0.308	0.379	0.353

- **Environmental chemistry:** Improved modeling of reaction pathways may aid in designing greener catalysts and processes.

NeurIPS Paper Checklist

The checklist is designed to encourage best practices for responsible machine learning research, addressing issues of reproducibility, transparency, research ethics, and societal impact. Do not remove the checklist: **The papers not including the checklist will be desk rejected.** The checklist should follow the references and follow the (optional) supplemental material. The checklist does NOT count towards the page limit.

Please read the checklist guidelines carefully for information on how to answer these questions. For each question in the checklist:

- You should answer [Yes], [No], or [NA].
- [NA] means either that the question is Not Applicable for that particular paper or the relevant information is Not Available.
- Please provide a short (1–2 sentence) justification right after your answer (even for NA).

The checklist answers are an integral part of your paper submission. They are visible to the reviewers, area chairs, senior area chairs, and ethics reviewers. You will be asked to also include it (after eventual revisions) with the final version of your paper, and its final version will be published with the paper.

The reviewers of your paper will be asked to use the checklist as one of the factors in their evaluation. While "[Yes]" is generally preferable to "[No]", it is perfectly acceptable to answer "[No]" provided a proper justification is given (e.g., "error bars are not reported because it would be too computationally expensive" or "we were unable to find the license for the dataset we used"). In general, answering "[No]" or "[NA]" is not grounds for rejection. While the questions are phrased in a binary way, we acknowledge that the true answer is often more nuanced, so please just use your best judgment and write a justification to elaborate. All supporting evidence can appear either in the main paper or the supplemental material, provided in appendix. If you answer [Yes] to a question, in the justification please point to the section(s) where related material for the question can be found.

IMPORTANT, please:

- Delete this instruction block, but keep the section heading "NeurIPS Paper Checklist",
- Keep the checklist subsection headings, questions/answers and guidelines below.
- Do not modify the questions and only use the provided macros for your answers.

1. Claims

Question: Do the main claims made in the abstract and introduction accurately reflect the paper's contributions and scope?

Answer: [Yes]

Justification: The Abstract and Introduction (Sec. 1) clearly enumerate the contributions—namely, explicit modeling of non-stationarity via Patch Fourier Transform, integration into an E(n)-equivariant GNN backbone, and extensive experiments validating performance—which match the scope and results presented.

Guidelines:

- The answer NA means that the abstract and introduction do not include the claims made in the paper.
- The abstract and/or introduction should clearly state the claims made, including the contributions made in the paper and important assumptions and limitations. A No or NA answer to this question will not be perceived well by the reviewers.
- The claims made should match theoretical and experimental results, and reflect how much the results can be expected to generalize to other settings.
- It is fine to include aspirational goals as motivation as long as it is clear that these goals are not attained by the paper.

2. Limitations

Question: Does the paper discuss the limitations of the work performed by the authors?

Answer: [Yes]

Justification: See Appendices D for limitation.

Guidelines:

- The answer NA means that the paper has no limitation while the answer No means that the paper has limitations, but those are not discussed in the paper.
- The authors are encouraged to create a separate "Limitations" section in their paper.
- The paper should point out any strong assumptions and how robust the results are to violations of these assumptions (e.g., independence assumptions, noiseless settings, model well-specification, asymptotic approximations only holding locally). The authors should reflect on how these assumptions might be violated in practice and what the implications would be.
- The authors should reflect on the scope of the claims made, e.g., if the approach was only tested on a few datasets or with a few runs. In general, empirical results often depend on implicit assumptions, which should be articulated.
- The authors should reflect on the factors that influence the performance of the approach. For example, a facial recognition algorithm may perform poorly when image resolution is low or images are taken in low lighting. Or a speech-to-text system might not be used reliably to provide closed captions for online lectures because it fails to handle technical jargon.
- The authors should discuss the computational efficiency of the proposed algorithms and how they scale with dataset size.
- If applicable, the authors should discuss possible limitations of their approach to address problems of privacy and fairness.
- While the authors might fear that complete honesty about limitations might be used by reviewers as grounds for rejection, a worse outcome might be that reviewers discover limitations that aren't acknowledged in the paper. The authors should use their best judgment and recognize that individual actions in favor of transparency play an important role in developing norms that preserve the integrity of the community. Reviewers will be specifically instructed to not penalize honesty concerning limitations.

3. Theory assumptions and proofs

Question: For each theoretical result, does the paper provide the full set of assumptions and a complete (and correct) proof?

Answer: [Yes]

Justification: All stated theoretical claims (Lemma 3.1 and Theorem 3.2) explicitly list their E(n)-equivariance assumptions and are accompanied by full proofs in Appendix A.1 and A.2.

Guidelines:

- The answer NA means that the paper does not include theoretical results.
- All the theorems, formulas, and proofs in the paper should be numbered and cross-referenced.
- All assumptions should be clearly stated or referenced in the statement of any theorems.
- The proofs can either appear in the main paper or the supplemental material, but if they appear in the supplemental material, the authors are encouraged to provide a short proof sketch to provide intuition.
- Inversely, any informal proof provided in the core of the paper should be complemented by formal proofs provided in appendix or supplemental material.
- Theorems and Lemmas that the proof relies upon should be properly referenced.

4. Experimental result reproducibility

Question: Does the paper fully disclose all the information needed to reproduce the main experimental results of the paper to the extent that it affects the main claims and/or conclusions of the paper (regardless of whether the code and data are provided or not)?

Answer: [Yes]

Justification: Section 4 details datasets, splits, ADF test procedures, baselines, optimizer settings, and hyperparameters; Appendix B.1 further describes implementation specifics and ADF-test preprocessing.

Guidelines:

- The answer NA means that the paper does not include experiments.
- If the paper includes experiments, a No answer to this question will not be perceived well by the reviewers: Making the paper reproducible is important, regardless of whether the code and data are provided or not.
- If the contribution is a dataset and/or model, the authors should describe the steps taken to make their results reproducible or verifiable.
- Depending on the contribution, reproducibility can be accomplished in various ways. For example, if the contribution is a novel architecture, describing the architecture fully might suffice, or if the contribution is a specific model and empirical evaluation, it may be necessary to either make it possible for others to replicate the model with the same dataset, or provide access to the model. In general, releasing code and data is often one good way to accomplish this, but reproducibility can also be provided via detailed instructions for how to replicate the results, access to a hosted model (e.g., in the case of a large language model), releasing of a model checkpoint, or other means that are appropriate to the research performed.
- While NeurIPS does not require releasing code, the conference does require all submissions to provide some reasonable avenue for reproducibility, which may depend on the nature of the contribution. For example
 - (a) If the contribution is primarily a new algorithm, the paper should make it clear how to reproduce that algorithm.
- (b) If the contribution is primarily a new model architecture, the paper should describe the architecture clearly and fully.
- (c) If the contribution is a new model (e.g., a large language model), then there should either be a way to access this model for reproducing the results or a way to reproduce the model (e.g., with an open-source dataset or instructions for how to construct the dataset).
- (d) We recognize that reproducibility may be tricky in some cases, in which case authors are welcome to describe the particular way they provide for reproducibility. In the case of closed-source models, it may be that access to the model is limited in some way (e.g., to registered users), but it should be possible for other researchers to have some path to reproducing or verifying the results.

5. Open access to data and code

Question: Does the paper provide open access to the data and code, with sufficient instructions to faithfully reproduce the main experimental results, as described in supplemental material?

Answer: [Yes]

Justification: Following NeurIPS instructions, we include our full codebase, detailed training and evaluation scripts, and step-by-step run instructions in the supplemental material.

- The answer NA means that paper does not include experiments requiring code.
- Please see the NeurIPS code and data submission guidelines (https://nips.cc/public/guides/CodeSubmissionPolicy) for more details.
- While we encourage the release of code and data, we understand that this might not be possible, so "No" is an acceptable answer. Papers cannot be rejected simply for not including code, unless this is central to the contribution (e.g., for a new open-source benchmark).
- The instructions should contain the exact command and environment needed to run to reproduce the results. See the NeurIPS code and data submission guidelines (https://nips.cc/public/guides/CodeSubmissionPolicy) for more details.
- The authors should provide instructions on data access and preparation, including how to access the raw data, preprocessed data, intermediate data, and generated data, etc.

- The authors should provide scripts to reproduce all experimental results for the new proposed method and baselines. If only a subset of experiments are reproducible, they should state which ones are omitted from the script and why.
- At submission time, to preserve anonymity, the authors should release anonymized versions (if applicable).
- Providing as much information as possible in supplemental material (appended to the paper) is recommended, but including URLs to data and code is permitted.

6. Experimental setting/details

Question: Does the paper specify all the training and test details (e.g., data splits, hyperparameters, how they were chosen, type of optimizer, etc.) necessary to understand the results?

Answer: [Yes]

Justification: Section 4 and Appendix B.2 enumerate data splits, batch sizes, learning rates, weight decay, number of epochs, optimizer choices, and layer configurations for each experiment.

Guidelines:

- The answer NA means that the paper does not include experiments.
- The experimental setting should be presented in the core of the paper to a level of detail that is necessary to appreciate the results and make sense of them.
- The full details can be provided either with the code, in appendix, or as supplemental material.

7. Experiment statistical significance

Question: Does the paper report error bars suitably and correctly defined or other appropriate information about the statistical significance of the experiments?

Answer: [Yes]

Justification: Results tables (e.g., Table 2, Table 3 and Table 4) report mean standard deviation over multiple runs, clearly indicating variability across seeds.

Guidelines:

- The answer NA means that the paper does not include experiments.
- The authors should answer "Yes" if the results are accompanied by error bars, confidence intervals, or statistical significance tests, at least for the experiments that support the main claims of the paper.
- The factors of variability that the error bars are capturing should be clearly stated (for example, train/test split, initialization, random drawing of some parameter, or overall run with given experimental conditions).
- The method for calculating the error bars should be explained (closed form formula, call to a library function, bootstrap, etc.)
- The assumptions made should be given (e.g., Normally distributed errors).
- It should be clear whether the error bar is the standard deviation or the standard error of the mean.
- It is OK to report 1-sigma error bars, but one should state it. The authors should preferably report a 2-sigma error bar than state that they have a 96% CI, if the hypothesis of Normality of errors is not verified.
- For asymmetric distributions, the authors should be careful not to show in tables or figures symmetric error bars that would yield results that are out of range (e.g. negative error rates).
- If error bars are reported in tables or plots, The authors should explain in the text how they were calculated and reference the corresponding figures or tables in the text.

8. Experiments compute resources

Question: For each experiment, does the paper provide sufficient information on the computer resources (type of compute workers, memory, time of execution) needed to reproduce the experiments?

Answer: [Yes]

Justification: See Appendices B.3 for compute-resource details and C.7 for execution times. Guidelines:

- The answer NA means that the paper does not include experiments.
- The paper should indicate the type of compute workers CPU or GPU, internal cluster, or cloud provider, including relevant memory and storage.
- The paper should provide the amount of compute required for each of the individual experimental runs as well as estimate the total compute.
- The paper should disclose whether the full research project required more compute than the experiments reported in the paper (e.g., preliminary or failed experiments that didn't make it into the paper).

9. Code of ethics

Question: Does the research conducted in the paper conform, in every respect, with the NeurIPS Code of Ethics https://neurips.cc/public/EthicsGuidelines?

Answer: [Yes]

Justification: We have reviewed and adhered to the NeurIPS Code of Ethics throughout—ensuring anonymity, proper data handling, and no conflicts with ethical guidelines.

Guidelines:

- The answer NA means that the authors have not reviewed the NeurIPS Code of Ethics.
- If the authors answer No, they should explain the special circumstances that require a deviation from the Code of Ethics.
- The authors should make sure to preserve anonymity (e.g., if there is a special consideration due to laws or regulations in their jurisdiction).

10. Broader impacts

Question: Does the paper discuss both potential positive societal impacts and negative societal impacts of the work performed?

Answer: [Yes]

Justification: We discuss potential benefits for drug discovery and green chemistry, as well as minimal misuse risk, in Appendix E.

- The answer NA means that there is no societal impact of the work performed.
- If the authors answer NA or No, they should explain why their work has no societal impact or why the paper does not address societal impact.
- Examples of negative societal impacts include potential malicious or unintended uses (e.g., disinformation, generating fake profiles, surveillance), fairness considerations (e.g., deployment of technologies that could make decisions that unfairly impact specific groups), privacy considerations, and security considerations.
- The conference expects that many papers will be foundational research and not tied to particular applications, let alone deployments. However, if there is a direct path to any negative applications, the authors should point it out. For example, it is legitimate to point out that an improvement in the quality of generative models could be used to generate deepfakes for disinformation. On the other hand, it is not needed to point out that a generic algorithm for optimizing neural networks could enable people to train models that generate Deepfakes faster.
- The authors should consider possible harms that could arise when the technology is being used as intended and functioning correctly, harms that could arise when the technology is being used as intended but gives incorrect results, and harms following from (intentional or unintentional) misuse of the technology.
- If there are negative societal impacts, the authors could also discuss possible mitigation strategies (e.g., gated release of models, providing defenses in addition to attacks, mechanisms for monitoring misuse, mechanisms to monitor how a system learns from feedback over time, improving the efficiency and accessibility of ML).

11. Safeguards

Question: Does the paper describe safeguards that have been put in place for responsible release of data or models that have a high risk for misuse (e.g., pretrained language models, image generators, or scraped datasets)?

Answer: [NA]

Justification: The work does not involve high-risk models or datasets requiring such safeguards.

Guidelines:

- The answer NA means that the paper poses no such risks.
- Released models that have a high risk for misuse or dual-use should be released
 with necessary safeguards to allow for controlled use of the model, for example by
 requiring that users adhere to usage guidelines or restrictions to access the model or
 implementing safety filters.
- Datasets that have been scraped from the Internet could pose safety risks. The authors should describe how they avoided releasing unsafe images.
- We recognize that providing effective safeguards is challenging, and many papers do not require this, but we encourage authors to take this into account and make a best faith effort.

12. Licenses for existing assets

Question: Are the creators or original owners of assets (e.g., code, data, models), used in the paper, properly credited and are the license and terms of use explicitly mentioned and properly respected?

Answer: [NA]

Justification: The paper does not use existing assets.

Guidelines:

- The answer NA means that the paper does not use existing assets.
- The authors should cite the original paper that produced the code package or dataset.
- The authors should state which version of the asset is used and, if possible, include a URL.
- The name of the license (e.g., CC-BY 4.0) should be included for each asset.
- For scraped data from a particular source (e.g., website), the copyright and terms of service of that source should be provided.
- If assets are released, the license, copyright information, and terms of use in the package should be provided. For popular datasets, paperswithcode.com/datasets has curated licenses for some datasets. Their licensing guide can help determine the license of a dataset.
- For existing datasets that are re-packaged, both the original license and the license of the derived asset (if it has changed) should be provided.
- If this information is not available online, the authors are encouraged to reach out to the asset's creators.

13. New assets

Question: Are new assets introduced in the paper well documented and is the documentation provided alongside the assets?

Answer: [NA]

Justification: The paper does not release new assets.

- The answer NA means that the paper does not release new assets.
- Researchers should communicate the details of the dataset/code/model as part of their submissions via structured templates. This includes details about training, license, limitations, etc.

- The paper should discuss whether and how consent was obtained from people whose asset is used.
- At submission time, remember to anonymize your assets (if applicable). You can either create an anonymized URL or include an anonymized zip file.

14. Crowdsourcing and research with human subjects

Question: For crowdsourcing experiments and research with human subjects, does the paper include the full text of instructions given to participants and screenshots, if applicable, as well as details about compensation (if any)?

Answer: [NA]

Justification: This work involves only physical-dynamics datasets and no human-subject studies.

Guidelines:

- The answer NA means that the paper does not involve crowdsourcing nor research with human subjects.
- Including this information in the supplemental material is fine, but if the main contribution of the paper involves human subjects, then as much detail as possible should be included in the main paper.
- According to the NeurIPS Code of Ethics, workers involved in data collection, curation, or other labor should be paid at least the minimum wage in the country of the data collector.

15. Institutional review board (IRB) approvals or equivalent for research with human subjects

Question: Does the paper describe potential risks incurred by study participants, whether such risks were disclosed to the subjects, and whether Institutional Review Board (IRB) approvals (or an equivalent approval/review based on the requirements of your country or institution) were obtained?

Answer: [NA]

Justification: No human-subject research is conducted in this study.

Guidelines:

- The answer NA means that the paper does not involve crowdsourcing nor research with human subjects.
- Depending on the country in which research is conducted, IRB approval (or equivalent) may be required for any human subjects research. If you obtained IRB approval, you should clearly state this in the paper.
- We recognize that the procedures for this may vary significantly between institutions and locations, and we expect authors to adhere to the NeurIPS Code of Ethics and the guidelines for their institution.
- For initial submissions, do not include any information that would break anonymity (if applicable), such as the institution conducting the review.

16. Declaration of LLM usage

Question: Does the paper describe the usage of LLMs if it is an important, original, or non-standard component of the core methods in this research? Note that if the LLM is used only for writing, editing, or formatting purposes and does not impact the core methodology, scientific rigorousness, or originality of the research, declaration is not required.

Answer: [NA]

Justification: The proposed methodology does not involve any large-language models.

- The answer NA means that the core method development in this research does not involve LLMs as any important, original, or non-standard components.
- Please refer to our LLM policy (https://neurips.cc/Conferences/2025/LLM) for what should or should not be described.